Adsorption technology and mechanism of As(III) and As(V) in wastewater by iron modified rice husk biochar

Shuyan Zang[1], Jinghan Shao[1], Congting Sun*,[2], Juan Wang[1] & Huafeng Zhou[1]

[1]Shenyang University of Chemical Technology, Shenyang 110142, China

[2]Liaoning University, Shenyang 110036, China

E-mail:congtingsun@lnu.edu.cn

Arsenic pollution has become a common phenomenon, which seriously endangers the environment and poses a great threat to human health. In this paper, a novel method has been developed for simultaneous removal of composite arsenic pollution based on the modified rice husk biochar as an efficient adsorbent. Iron modified rice husk biochar (MRHB) adsorbent has been prepared using rice husk as raw material, $NaHCO_3$ as pore expander, $FeCl_3 \cdot 6H_2O$ as modifier and NaOH as precipitant. The adsorption characteristics of MRHB for As(III) and As(V) has been investigated on the basis of batch experiments. X-ray diffraction, scanning electron microscopy, and Fourier Transform Infrared were carried out to characterize the composition and structure of MRHB. The results show that the arsenic concentration of 1.0 mg/L, adsorbent dosage of 1.0 g/L, the maximum removal rates of As(III) and As(V) are 99.88% and 99.93% at *p*H of 5. The adsorption performance of MRHB for As(V) and As(V) fits well to the pseudo-second-order kinetic model, indicating that the chemisorption control plays a dominant role in adsorption process. Results from this study demonstrated the promise of MRHB in application as an efficient and environmentally friendly adsorbent for composite arsenic pollution.

Keywords：Adsorption, Arsenate, Arsenite, Iron, Rice husk biochar

Arsenic (As) is a persistent, bio-accumulative and toxic substance which has already been taken as the first group of carcinogens by the International Agency for Research on Cancer. It is widely distributed in the environment owing to the discharging of anthropogenic sources into water or soil[1-3]. In ground water and surface water, the main valence states of arsenic species are trivalent As(III) and pentavalent As(V), respectively[4,5], in which As(III) is more toxic and mobile than As(V)[6]. Long-term exposure to arsenic-contaminated drinking water will lead to potential human health hazards, including skin cancer, stomach cancer, respiratory tract cancer and bladder cancer, neurological disorders, respiratory tract conditions, as well as affect cardiovascular and nervous systems, even at low levels of exposure[7-9]. Due to its high toxicity and accumulation, the World Health Organization (WHO) has professed that the maximum concentration of arsenic in drinking water is 10 μg/L[10-12]. In order to meet the strict drinking water standards, it is necessary to develop an efficient, low-cost and no secondary pollution treatment process for the removal of compound arsenic contaminated wastewater.

At present, there are many methods for arsenic pollution treatment[13], such as precipitation[14], membrane separation[15], ion exchange[16], adsorption[17], and so on. Among these methods, adsorption method has been widely used in wastewater treatment with the advantages of low cost, high removal rate, easy treatment, convenient operation and relatively mature[18-20]. The commonly used material for adsorption method is biochar. Biochar is a kind of highly aromatic solid products rich in carbon made from agricultural and forestry wastes under oxygen limiting conditions. It has been attract much attention due to its architectural advantage such as large specific surface area, abundant pore and various functional groups[21-23]. However, the arsenic adsorption capacity of original biochar is low, and biochar was modified by iron in order to improve its adsorption capacity[24]. The modified biochar possesses improved pore structure, larger specific surface area, and anticipatory surface functional groups that can be chemically combined with pollutants[25,26]. The modified biochar has been widely used for heavy metal removal in wastewater treatment[27,28]. Previous studies show that the modified

biochar has an excellent adsorption capacity for As(V), however, the adsorption ability for more toxic As(III) is unsatisfactory[29,30]. Therefore, a low-cost and safe modified biochar adsorbent is needed to removal As(III) efficiently.

China is extremely rich in rice husk resources. The pyrolysis of waste rice husk to prepare biochar can not only realize the resource utilization of solid waste, but also reduce the environmental problems caused by rice husk accumulation[31,32]. From the view of resource utilization of solid waste, rice husk biochar may become a promising adsorption material for adsorption and removal of arsenic in water treatment. Until now, there are few reports by iron modified rice husk. In this study, we prepared an iron loaded rice husk biochar that can serve as an adsorbent to removal both As(III) and As(V) within short time. In order to examine the adsorption capacity of iron loaded rice husk biochar for arsenic adsorption in wastewater, the effects of initial pH value, temperature, adsorbent dosage, and adsorption kinetics were studied in details. Furthermore, the adsorption mechanism was also preliminarily discussed. The present study may provide a promising pathway for wastewater treatment.

Experimental Section

Materials

The chemical reagents used in this work were analytical grade. RHB was prepared by pyrolyzing a certain quality of rice husk in a muffle furnace at 350°C for 3 h and then passing a 200 mesh sieve. 4.0 g rice husk biochar and 100 mL saturated NaHCO$_3$ solution were put into a beaker, and the mixture was dispersed by ultrasound for 5 min and stirring for 30 min. Thereafter, the obtained solid is dried in the oven, and the dried solid was activated by heating at 350°C for 3 h in muffle furnace. 3.0 g activated RHB was added into 100 mL 1 mol/L FeCl$_3$ solution. After ultrasonic dispersion for 5 min, 1 mol/L NaOH solution was slowly pour into the mixture until the formation of precipitation. The as-prepared suspension was finally washed with deionized water and dried at 100°C for 12 h to obtain the Fe loaded RHB (MRHB).

Batch adsorption experiments

In this study, batch experiments were carried out in order to investigate the adsorption ability of MRHB for both As(III) and As(V) pollutants. At room temperature, 0.2 g MRHB was added to 200 mL mixed solution with 1 mg/L As(III) and 1 mg/L As(V). The pH value of the solution was adjusted with 1 mol/L NaOH/HCl and retained an unchanged value during the adsorption process. The adsorption experiments were carried out at 25±1°C, and the performances of the adsorbent were measured by the removal rate of As(III) and As(V). In adsorption experiments, the influences of solution pH, solution temperature, and adsorbent dose in removal rate of As(III) and As(V) from contaminated water were considered and analyzed.

The adsorption capacity (q, mg/g) and removal rate (R, %) of As(III) and As(V) were calculated as following equations[33] :

$$R(\%) = \frac{(C_0 - C_e)}{C_0} \times 100\% \qquad \cdots (1)$$

$$q_e = \frac{(C_0 - C_e)V}{m} \qquad \cdots (2)$$

where R is the removal rate of As(III) and As(V) in the solution (%), C_0 and C_e are the initial and equilibrium concentrations (mg/L) of As(III) and As(V) in the solution, respectively, V is the volume (L) of the solution and m is the mass (g) of the adsorbent.

Adsorption kinetics

The adsorption rate acts as an important factor for arsenic removal. Batch experiments were carried out in order to obtain the adsorption equilibrium time at 25±1°C. In particular adsorption test, the adsorbent dose was 0.2 g for 200 mL arsenic solution with 1 mg/L As(III) and 1 mg/L As(V). The solution pH value was fixed at 5.0±0.2 during the adsorption process. Then, the mixture was shaken on a platform shaker with an agitation speed of 180 rpm. Approximately, 1 mL aliquots were taken from the vessel at selected reaction time intervals (0.083, 0.167, 0.25, 0.5, 1, 2, 4, 8, 12, and 24 h) and then filtered through a 0.22 μm membrane filter. Three replicates were performed for each treatment. Control experiments were operated in the same conditions except without adsorbent.

Arsenic adsorption edges

In order to investigate the influence of pH on arsenic adsorption by MRHB, batch experiments were

carried out at different *p*H values, in which 0.1 g adsorbent sample was added to 100 mL arsenic solution with 1 mg/L As(III) and 1 mg/L As(V). The mixtures with the *p*H value of 3.0, 5.0, 6.0, 7.0, 8.0 and 9.0 respectively were sharked on a platform shaker. It is notable that the *p*H values kept unchanged during the adsorption process. Other conduct was the same to above description.

Reaction temperature

In order to study the influence of temperature on arsenic adsorption by MRHB, the adsorption reactions in which 0.1 g adsorbent sample was added to 100 mL arsenic solution with 1 mg/L As(III) and 1 mg/L As(V) were carried out at the temperature of 15, 20, 25, 30 and 40°C, respectively. The solution *p*H value was fixed at 5.0±0.2 during the adsorption process. Other conduct was the same to above description.

Adsorbent dosage

Furthermore, different MRHB doses were added to 100 mL arsenic solution with 1 mg/L As(III) and 1 mg/L As(V) in order to obtain the optimum adsorbent dosage. In arsenic solution, MRHB concentrations were 0.1, 0.2, 0.4, 0.6, 0.8, 1.0, 1.2 g/L. Other conduct was the same to above description.

Analytical methods

The concentrations of As(III) and total inorganic arsenic in solution were measured using a hydride-generation atomic fluorescence spectrophotometer (AFS-HG Hydride generation, AFS-2202E) with a detection limit of 0.1 µg/L, and duplicate analyses agreed within 5%, according to previously reported procedures[34,35]. The concentration of As(III) was determined initially by AFS-HG. Thereafter, As(V) was reduced to As(III) by thiourea and ascorbic acid (5 g thiourea and 5 g ascorbic acid in 100 mL H$_2$O), and the total inorganic arsenic content was determined by AFS-HG and the concentration of As(V) was calculated by subtraction[36,37]. The phase and morphology of the adsorbent were characterized by X-ray diffraction (XRD, D8 Quest), Fourier Transform Infrared (FTIR, NICOLET6700), and scanning electron microscopy (SEM, JSM-636OLV).

Results and Discussion

Characterization and analysis

As shown in Fig. 1(a), RHB has flocculent porous structure, loose surface and large specific surface area. The microstructure characteristics of RHB can provide amount loaded sites for iron precipitations. From SEM images, it can be found that iron precipitations in the form of iron-based complex, such as iron(III)-oxy ohydroxides[30] are distributed on both inside and outside surfaces of MRHB, resulting in the compact surface for MRHB [Fig. 1(b)]. Fig. 1(c) shows the microstructure of rice husk biochar after arsenic adsorption. Because the biochar sample has a smooth surface morphology, it means that the iron precipitations on the biochar may participate to the reaction with As(III) and As(V) during adsorption process.

In order to further clarify the compositions and functional groups of MRHB, IR spectroscopy was carried out for RHB, MRHB, and As-MRHB. As shown in Fig. 2, there is no significant difference between the functional groups on RHB, MRHB, and As-MRHB. The wider absorption bands at 3380, 3371, and 3404 cm^{-1} are assigned to the associated −OH group[28]. The difference among these absorption bands for RHB, MRHB, and As-MRHB is peak intensity, in which the peak intensity of RHB and As-MRHB are weaker than that of MRHB. The absorption band at 2930 cm^{-1} is assigned to the symmetric stretching vibration of C−H bond, the absorption bands at 1610 cm^{-1} is assigned to the asymmetric stretching vibration of C−C bond, and the absorption bands at 1407 cm^{-1} is assigned to the asymmetric stretching vibration of C−O bond. Compared with RHB, MRHB showed new vibration bands at 1705 and 587 cm^{-1}. The absorption bands at

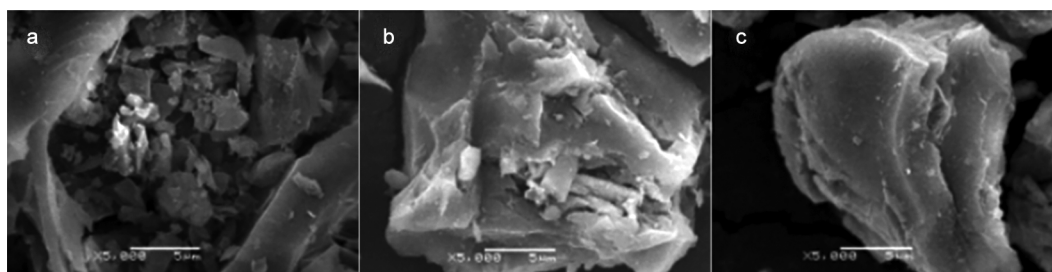

Fig. 1 — SEM of RHB (a), MRHB (b), and As-MRHB (c)

1705 cm^{-1} is assigned to the asymmetric stretching vibration of carbonyl bond, and the absorption bands at 587 cm^{-1} is assigned to the asymmetric stretching vibration of Fe–O bond. It implies that Fe was successfully loaded on rice husk biochar. These oxygen-containing functional groups are electron donating groups, which can strengthen the electrostatic attraction of activated carbon and facilitate the adsorption capacity. After the absorption of arsenic by MRHB, some absorption bands disappeared, and the peak intensity become weaker, which may be induced by the formation of Fe-As co-precipitations on MRHB surface covering the functional groups on MRHB surface.

XRD was used to characterize the phase structures of RHB, MRHB, and As-MRHB. A broad diffraction peak around $2\theta = 22.36°$ is shown in XRD pattern of RHB, corresponding to the characteristic peak of SiO$_2$, indicating an amorphous state RHB with a large amount of cellulose structure in rice husk and without any crystal attached to the surface (Fig. 3). There is no obvious diffraction peak of carbon for MRHB, which indicates the surface of carbon has been covered by modified iron, but good crystal have not formed yet[38]. For MRHB, there is nearly no obvious diffraction peak in XRD pattern, which is obviously different from that of RHB. Particularly, the diffraction peaks around $2\theta = 36.37°$ and $38.04°$ can be assigned to Fe(OH)$_3$, indicating that the biochar is loaded with Fe(OH)$_3$. It can therefore be deduced that the iron hydroxide crystal has been precipitated on the surface of rice husk biochar during the modification process. The precipitation of Fe would provide new active sites for MRHB adsorption[39], and act as a key factor that enhances the adsorption and removal capacity of arsenic for rice husk biochar. The XRD patterns of the MRHB before and after As(III) and As(V) adsorption were slightly different (Fig. 3).

Adsorbent performance evaluation

Effect of reaction time

In order to testify the adsorption capacity of MRHB in the removal of As(III) and As(V), the reaction time-removal rate relationship was studied. As shown in Fig. 4, it can be found that the removal rates of As(III) and As(V) gradually increase with increasing the time, and the removal rate increases rapidly within 2 h in the initial stage. MRHB exhibits an excellent adsorption capacity for As(III) and As(V), and the removal rate of As(III) and As(V) are higher than 90%. Moreover, both As(III) and As(V) reached adsorption equilibrium at about 2 h, and then

the removal rate increased slowly with increasing the time. After 2 h, there is nearly no change in the As(III) removal rate by MRHB, implying the most adsorption capacity of MRHB for As(III). Therefore, 2h is enough to reach the adsorption equilibrium of As(III) and As(V) combined pollution by MRHB.

Effect of pH

The *p*H value of solution is an important factor that may influence the electric charge distribution at the solid-liquid interface system. Generally speaking, the *p*H value will affect the surface charge of the adsorbent and the form of arsenic[40]. The relationship between the removal rate of As(III) and As(V) by
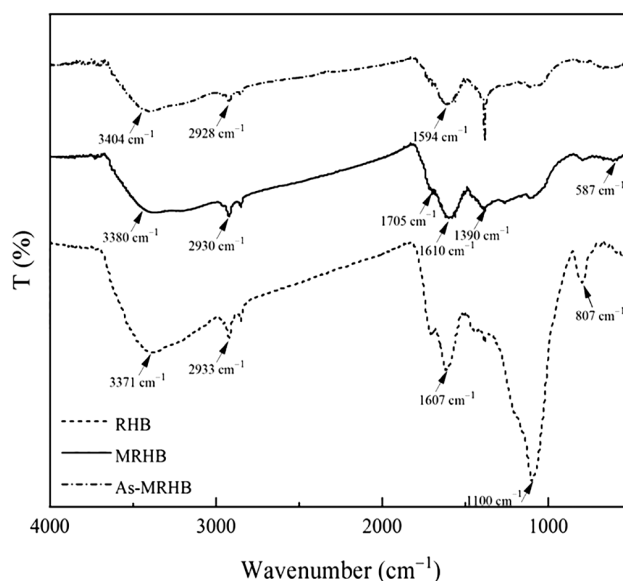

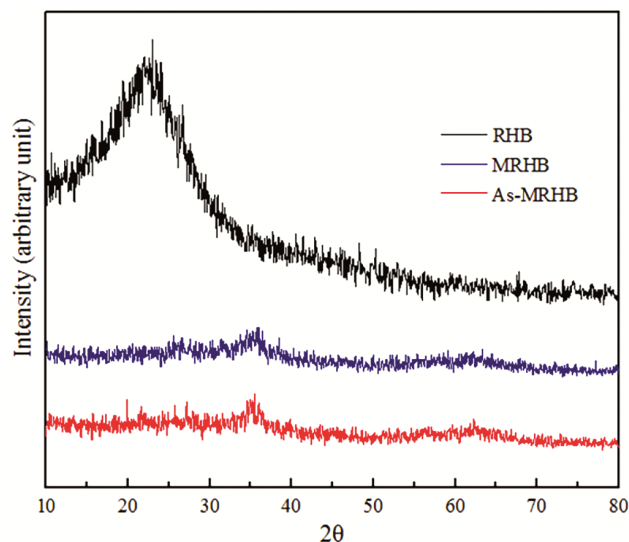Fig. 2 — FTIR spectra of RHB, MRHB, and As-MRHB.
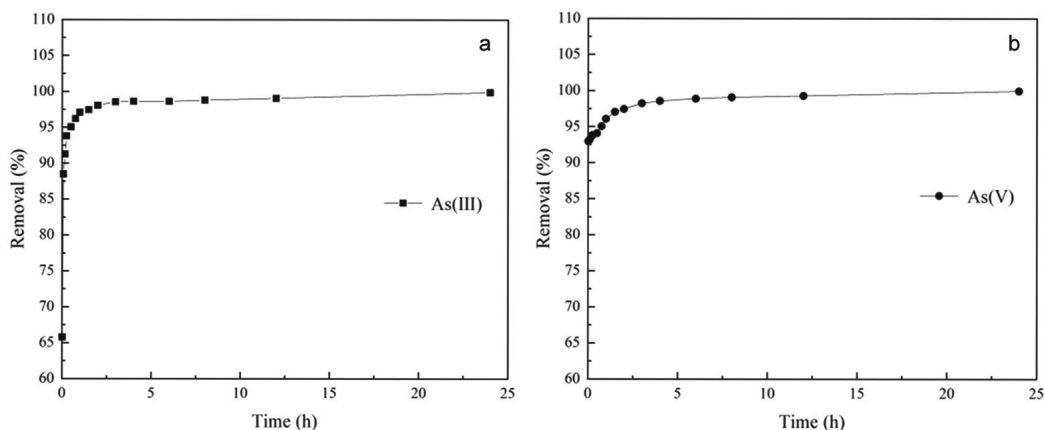

Fig. 3 — XRD patterns of RHB, MRHB, and As-MRHB.

Fig. 4 — Effect of adsorption time on the removal of As(III) (a) and As(V) (b) composite solution.

MRHB and the solution pH value is shown in Fig. 5. With increasing the solution pH value from 3 to 9, the removal rates of As(III) and As(V) in the composite solution initially increased and then decreased. The removal rates of As(III) and As(V) were the highest at pH 5, which can reach 99%. According to the phase diagrams of As(III) and As(V), it can be found that As(III) mainly exists in the form of $H_2AsO_3^-$ and As(V) mainly exists in the form of $H_2AsO_4^-$ at pH 5, both of As(III) and As(V) species are negatively charged. Under this condition, the removal rate of both As(III) and As(V) reaches the maximum value. This is due to the fact that the adsorbent MRHB measured in the experiment is positively charged at pH=5. Positive MRHB favours to attract the negative $H_2AsO_3^-$ and $H_2AsO_4^-$, resulting in the higher adsorption rate for both As(III) and As(V). With further increasing the solution pH value, the isoelectric point of MRHB is no longer larger than the solution pH, and MRHB has negatively charged surfaces. Consequently, the adsorption rate gradually decreases owing to the repulsive interaction between negative arsenic species and negative MRHB.

Effect of temperature

As shown in Fig. 6, there is not obvious change in the removal rate of As(III) and As(V) by MRHB under different reaction temperatures. When the reaction temperature is 25℃, the removal rate of As(III) reaches the maximum value as high as 99%. Similarly, the removal rate of As(V) also reaches the maximum value as high as 99% at 25℃. From the view of both energy consumption and time arrangement, 25℃ is selected as the optimal condition for the adsorption of MRHB adsorbent in this study.
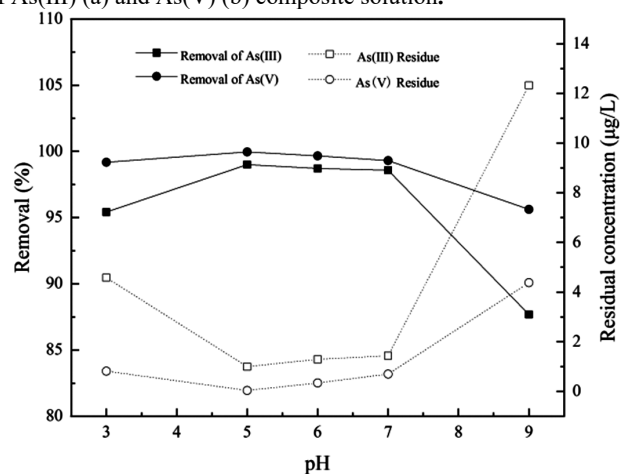

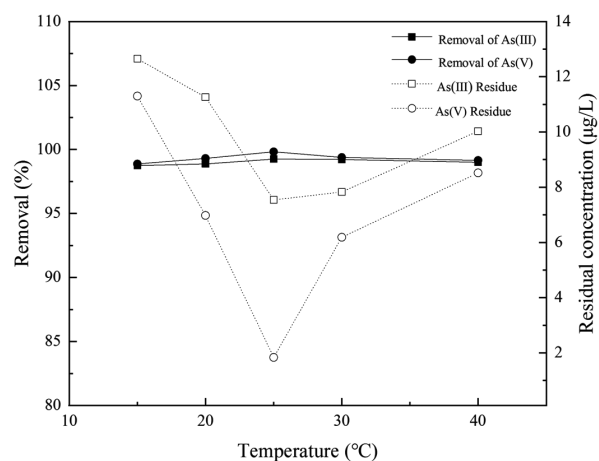Fig. 5 — Effect of pH on the adsorption of As(III) and As(V) by MRHB.

Fig. 6 — Effect of reaction temperature on the adsorption of As(III) and As(V) by MRHB

Effect of adsorbent dosage

Previous study shows that the removal of arsenic is strongly affected by the dosage of the adsorbent[28]. In order to check the optimal dosage of the adsorbent for

the removal of As(III) and As(V), a batch of experiments was carried out in this study. With increasing the adsorbent dosage, the removal rate of As(III) and As(V) pollutants gradually increases in Fig. 7. For As(III), it can be observed that the removal rate increased rapidly with increasing adsorbent dosage, however, the removal rate of As(V) remains nearly unchanged with further increasing adsorbent dose. Moreover, the removal rate of As(V) is higher than that of As(III). Once the MRHB dosage was larger than 1.0 g/L, the removal rates of As(III) and As(V) by MRHB are basically unchanged, both reaching more than 98%. Therefore, considering the removal rate of As(III) and As(V) and the adsorption capacity of adsorbent, the optimal dosage of MRHB is 1.0 g/L.

Adsorption kinetics

Kinetic is an important criterion for the design of adsorption system because it determines the equilibrium time. In order to further explore the adsorption characteristics of MRHB in As(III) and As(V) pollutant solution, the pseudo-first order and pseudo-second-order rate equations were used to fit the kinetic data in As(III) and As(V) adsorption experiment. The pseudo-first order and pseudo-second-order rate equations are following:

Pseudo-first order dynamics model:

$$\ln(q_e - q_t) = \ln q_e - k_1 t \qquad \cdots (3)$$

Pseudo-two order kinetic model:

$$\frac{t}{q_t} = \frac{1}{k_2 q_e^2} + \frac{t}{q_e} \qquad \cdots (4)$$

in which q_t and q_e respectively are the adsorption amount of As(III) and As(V) at time t and adsorption equilibrium (mg/g), t is the adsorption time (h), k_1 is the rate constant in the quasi-first order kinetic model (1/h), and k_2 is the rate constant in the quasi-two order kinetic model (g/mg/h).

It can be seen from Table 1 that the correlation coefficient R^2 of the Pseudo-first-order kinetic model is small and the fitting degree is very low, so the

adsorption of As(III) and As(V) by MRHB does not obey to the Pseudo-first-order kinetic equation (Fig. 8). The correlation coefficient R^2 of the quasi-second-order kinetic models of As(III) and As(V) is larger than 0.999, which has a high fitting degree. According to the numerical comparison of R^2, the Pseudo-second-order kinetic fitting of the adsorption process of As(III) and As(V) in the solution by MRHB is better than the Pseudo-first-order kinetic
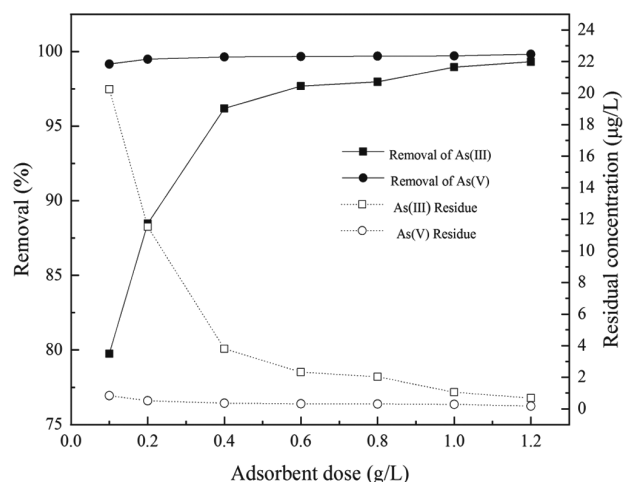

Fig. 7 — Effect of the adsorbent dosage on arsenic removal respectively for As(III) and As(V).
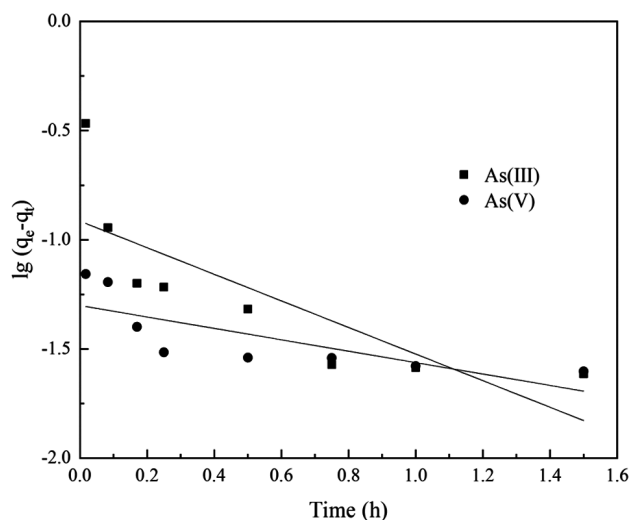

Fig. 8 — First-order rate model of 1 mg/L As(III) and mg/L As(V) with 1 g/L MRHB and room temperature.

Table 1— As(III) and As(V) kinetic parameters

As	Pseudo-first-order Kinetics			Pseudo-second-order Kinetics		
	R^2	q_e(mg/g)	K_1(g/mg.h)	R^2	q_e(mg/g)	K_2(g/mg.h)
As(III)	0.6569	0.5362	5.32	0.9999	0.9988	187.34
As(V)	0.5993	0.2213	5.73	0.9999	0.9993	214.72

Table 2 — Comparison of uptake capacity, *p*H, best-ftted isotherm model constants of As(III) and As(V) with other studied adsorbents

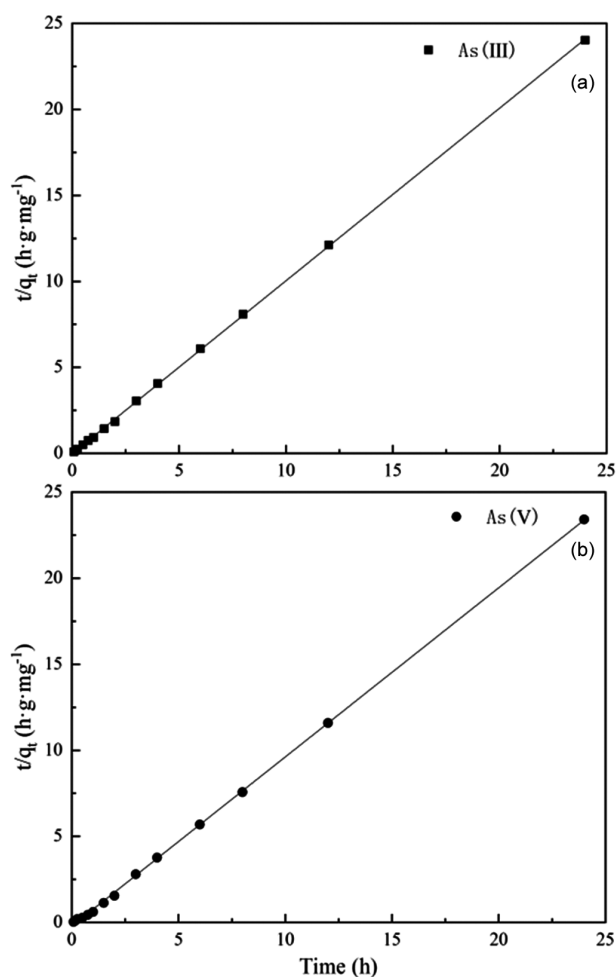| Adsorbent	Arsenic species	*p*H	Model used to calculate uptake capacity	Uptake capacity (mg/g)	References
Cassiafistula (golden shower) biochar	As (III)	6.0	Langmuir	0.78	[29]
	As (V)	2.0		0.42	
Waste biomass of Citrus limetta (peel and pulp)	As (III)	3.0	Langmuir	0.714	[41]
	As (V)			2.0	
Coal fly ash	As (III)	5.0	Langmuir	0.233	[36]
	As (V)			0.667	
Rice husk biochar	As (III)	5.0	Langmuir	0.9988	this study
	As (V)			0.9993	

Fig. 9— Pseudo-second-order rate model of 1 mg/L As(III) (a) and 1 mg/L As(V) and (b) with 1 g/L MRHB and room temperature.

fitting, indicating that the adsorption process is mainly controlled by chemical action. The q_e of As(III) and As(V) obtained from the pseudo-second-order equation model respectively were 0.998 and 0.9993 mg/g (Fig.9). Table 2 shows the comparison of bio-sorption capacity in the current work and in previous works.

Conclusion

In this study, a low-cost rice husk biochar modified by $FeCl_3$ has been developed as the high-effective adsorbent for the simultaneous removal of As(III) and As(V) composite pollution solutions. The condition of arsenic removal was optimized by examining different influence factors, including equilibrium time, *p*H value, temperature, and adsorbent dosage. Under the optimized adsorption condition for MRHB, the adsorption capacities of adsorbent for As(III) and As(V)can respectively reached 0.9988 and 0.9993 mg/g, corresponding to the removal rates of 99.88% and 99.94%, and its residual concentration has reached the national emission standard. The adsorption mechanism of arsenic compound pollution was consistent with the pseudo-second-order kinetic model, indicating that the adsorption process is dominated by chemisorption. Our results demonstrate the ability of modified biochar in the treatment of composite arsenic contaminations and provide a promising materials design idea for rapid removal of heavy metals in applications.

References

1   Hao L L, Liu M Z, Wang N N & Li G J, *RSC Adv*, 8 (2018) 39545.
2   Jomova K, Jenisova Z, Feszterova M, Baros S, Liska J, Hudecova D, Rhodes C J & Valko M, *J Appl Toxicol*, 31 (2011) 95.

3   Asere T G, Stevens C V & Laing G D, *Sci Total Environ*, 676 (2019) 706.
4   Toxicology C O, Council N & Sciences N, *National Academies Press*, (2001).
5   Pokhrel D & Viraraghavan T, *Water Air Soil Poll*, 173 (2016) 195.
6   Wongrod S, Simon S, Hullebusch E V, Lens P & Guibaud G, *Bioresour Technol*, 275 (2019) 232.
7   Tahmasebpoor M, Sanaei L, Khatamian M & Divband B, *Mech Eng*, 5 (2020) 1.
8   Mohanty D, *Water Air Soil Poll*, 228 (2017) 381.
9   Sharma V K & Sohn M, *Environ Int*, 35 (2009) 743.
10   Xin H, Ding Z H, Zimmerman A R, Wang S S & Gao B, *Water Res*, 68 (2015) 206.
11   Sun T Y, Shi Z F, Zhang X P, Wang X H, Zhu L H & Lin Q, *J Alloys Compd*, 808 (2019) 151689.
12   Shukla S P, *Indian J Chem Technol*, 27 (2021) 479.
13   Hussain M, Imran M, Abbas G, Shahid M & Islam A U, *Environ Geochem Hlth*, 42 (2019) 2519.
14   Jia Y F, Xu L Y, Fang Z & Demopoulos G P, *Environ Sci Technol*, 40 (2006) 3284.
15   Seidel A, Waypa J J & Elimelech M, *Environ Eng Sci*, 18 (2001) 105.
16   Mondal P, Balomajumder C & Mohanty B, *Clean-Soil Air Water*, 35 (2017) 255.
17   Sanyang M L, Ghani W, Idris A & Ahmad M B, *Desalin Water Treat*, 57 (2016) 3674.
18   Danish M I, Awan M A, Qazi I A, Zeb A, Habib A & Khan Z, *J Nanomate*, 32 (2013) 4979.
19   Yap M W, Mubarak N M, Sahu J N & Abdullah E C, *J Ind Eng Chem*, 45 (2017) 287.
20   Niazi N K, Bibi I, Shahid M, Ok Y S, Burton E D, Wang H L, Shaheen S M, Rinklebe J, Lüttge A, *Environ Pollut*, 232 (2018) 31.
21   Das O & Sarmah A K, *Sci Total Environ*, 512 (2015) 682.
22   Jiang J, Xu R K, Jiang T Y & Li Z, *J Hazard Mater*, 229 (2012) 145.
23   Liu S, Xu W H, Liu Y G, Tan X F, Zeng G M, Li X, Liang J, Zhou Z, Yan Z L & Cai X X, *Sci Total Environ*, 592 (2017) 546.
24   Pehlivan E, Tran T H, Ouédraogo W K I, Schmidt C, Zachmann D & Bahadir M, *Fuel Process Technol*, 106 (2013) 511.
25   Li H B, Dong X L, Silva, E B, de Oliveira L M, Chen Y S & Ma L Q, *Chemosphere*, 178 (2017) 466.
26   Huang D L, Zeng G M, Feng C L, Hu S, Jiang X Y, Tang L, Su F F, Zhang Y, Zeng W & Liu H L, *Environ Sci Technol*, 42 (2008) 4946.
27   Ahmed M B, Zhou J L, Ngo H H, Guo W S & Chen M F, *Bioresource Technol*, 214 (2016) 836.
28   He R Z, Peng Z Y, Lyu H H, Huang H, Nan Q & Tang J C, *Sci Total Environ*, 612 (2018) 1177.
29   Alam M A, Shaikh W A, Alam M O, Bhattacharya T, Chakraborty S, Show B & Saha I, *Appl Water Sci*, 8 (2018) 198.
30   Zang S Y, Zuo Y Y, Wang J, Liu X M, Gomez M A & Wei L, *Acta Geochimica*, 40 (2021) 409.
31   Dos Reis G S D, Wilhelm M, de Almeida Silva T C, Rezwan K, Sampaio C H, Lima E C & de Souza S M G U, *Appl Therm Eng*, 93 (2016) 590.
32   Gong X M, Huang D L, Liu Y G, Zeng G M, Wang R Z, Wei J J, Huang C, Xu P, Wan J & Zhang C, *Bioresource Technol*, 253 (2018) 64.
33   Agrawal S & Singh N B, *Indian J Chem Technol*, 23 (2016) 374.
34   Xu L Y, Zhao Z X, Wang S F, Pan R R & Jia Y F, *Water Res*, 45 (2011) 6781.
35   Yuan Z D, Wang S F, Ma X, Wang X, Zhang G Q, Jia Y F & Zheng W, *Environ Sci Pollut Res Int*, 24 (2017) 26534.
36   Guo S Y, Feng B & Zhang H F, *J Fluoresc*, 21 (2011) 1281.
37   Wang Y L, Wang S F, Zhang G Q, Wang X, Zang S Y & Jia Y F, *Desasalin Water Treat*, 151 (2019) 242.
38   Yuan S N, Hong M F, Li H, Ye Z H, Gong H B, Zhang J Y, Huang Q Y & Tan Z X, *Sci Total Environ*, 733 (2020) 139320.
39   Franco D S P, Tanabe E H, Bertuol D A, Dos Reis G S, Lima É C & Dotto G L, *Water Sci Technol*, 75 (2016) 296.
40   You N, Wang X F, Li J Y, Fan H T & Zhang Q, *J Ind Eng Chem*, 70 (2018) 346.
41   Verma L, Siddique M A, Singh J & Bharagava R N, *J Environ Manage*, 250 (2019) 109452.